ELSEVIER

Pattern Recognition Letters 20 (1999) 1431–1438

Pattern Recognition Letters

www.elsevier.nl/locate/patrec

A fuzzy hyperspectral classifier for automatic target recognition (ATR) systems

Sameh M. Yamany [a], Aly A. Farag [a,*], Shin-Yi Hsu [b]

[a] *Department of Electrical Engineering, Computer Vision and Image Processing Laboratory, University of Louisville, Louisville, KY 40292, USA*

[b] *Susquehanna Resources and Environment, Inc., Binghamton, NY, USA*

Abstract

In this paper we present a fuzzy system based hyperspectral classifier for automatic target identification. The system is based on partitioning the spectral band space into clusters using a modified fuzzy C-Means clustering algorithm. Classification of each pixel is then carried out by calculating its fuzzy membership in each cluster. The results showed that the fuzzy hyperspectral classifier is successful in target identification using materials spectrum. Also it provides a fuzzy identification value that can be used later on in the decision-making stage of automatic target recognition (ATR) systems. © 1999 Elsevier Science B.V. All rights reserved.

Keywords: Fuzzy C-Means; Hyperspectral classification; Target identification

1. Introduction

Automatic target recognition (ATR) is an important task in image exploitation, but it is an extremely complex process. ATR systems should be able to *detect*, *classify*, *recognize* and/or *identify* targets in an environment where the background is *cluttered* and targets are at long distances and may be partially occluded, degraded by weather, or camouflaged. This work is part of a research that focuses on solving problems of target *detection*, *classification*, and *identification* using a multi-sensor suite, including hyperspectral visible to short-wave infrared sensors, a stereo imaging system, and a data link approach. Hsu and Huang (1997) showed that hyperspectral sensing in the visible and short-wave infrared range (0.39–2.5 μm range) using a reflectance-based spectral signature is highly stable for material identification in the daytime. A hyperspectral thermal sensing system may also deliver the same results for target detection at night. Yet, even in a laboratory based controlled environment, variations can exist in the hyperspectral material signatures. Therefore, the classification results based on a single spectral signature library are not reliable and thus not representative. For this reason, a fuzzy logic classification methodology is more plausible for the detection and classification task. The method is based on partitioning the spectral band space into clusters, using the Fuzzy-C-Means (FCM) algorithm, where each cluster represents one of the given spectral signatures in the library. Classification of each pixel signature is then carried out by calculating its fuzzy membership in each class. The

* Corresponding author.
E-mail address: farag@cairo.spd.louisville.edu (A.A. Farag)

0167-8655/99/$ - see front matter
PII: S0167-8655(99)00116-6

FCM algorithm is an unsupervised technique that uses an iterative algorithm with an objective function to estimate cluster centers and membership values of each pixel element with each cluster. Mohamed et al. (1998) introduced a Modified Fuzzy C-Means (M-FCM) algorithm to reduce the sensitivity of the FCM to noise. This technique was used in medical image segmentation. The technique, inspired by the Markov Random field, uses neighboring pixels membership values to enhance the clustering results. In this work, we used the M-FCM to construct a hyperspectral fuzzy classifier.

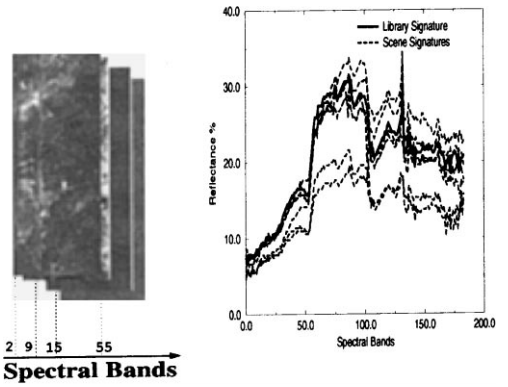

Fig. 1. Original hyperspectral stack and an example of the variation in spectral signatures for the same material.

2. Hyperspectral imaging

Hyperspectral imaging is the simultaneous acquisition of images in hundreds of narrow, contiguous, spectral bands. The development of airborne hyperspectral imaging spectrometers has provided an important tool for identifying materials of unknown objects and structures in remote sensing operations. Among the hyperspectral sensors used are the Airborne Visible/Infrared Imaging Spectrometer (AVIRIS) (Vane et al., 1993) and the Hyperspectral Digital Imagery Collection Experiment (HYDICE) (Basedow et al., 1995). These two sensors obtain over two hundred spectral measurements per spatial location over the spectral range 0.4–2.5 μm. There are many possible targets and backgrounds in an imaged scene. These various targets may have a variety of signatures in the various spectral regions. Our focus in this research is to detect possible Regions of Interest (ROIs) in terms of man-made versus natural material by matching each pixel in the scene against a set of spectral signatures in a given spectral library. However, as shown in Fig. 1, the signatures generated using an airborne hyperspectral imaging spectrometer vary with time of day, season, solar loading, history, geographical location, operational status, aspect of presentation, friction and atmospheric conditions (Ratches et al., 1997; Slater and Healey, 1998). Also, imaging sensors are noisy in nature and this contributes to variation in the pixel intensities for the same material at the same spectral band. This variation could affect the classification results by either giving a false identification value or by ignoring part of the object to be identified. This can be very critical when the object is small or when imaging is done at high altitudes.

A number of approaches have been considered for multispectral data analysis (Chulhee and Landgrebe, 1993; Landgrebe, 1999). These approaches include: deterministic approaches, stochastic models, AI techniques, fuzzy logic, neural networks and others. Deterministic approaches tend to be the most easy to implement and understand. However, deterministic methods are not as powerful, and may have other disadvantages, such as being more sensitive to noise than is necessary. Landgrebe (1999) analyzed the advantages of the stochastic or random process approach. This approach, due to its maturity, has a large collections of tools of pivotal usefulness in the analysis of multispectral data. However, in remote sensing, there are often a large number of features available, but the number of training samples is limited due to the difficulty and expense in labeling them. This leads to inaccurate estimates of the covariance matrix which consequently leads to lowered classification accuracy. Fuzzy logic approaches have been used for analyzing multispectral data (Burrough et al., 1992). Among the fuzzy logic techniques, the FCM technique has the advantage of clustering data without the need for an a priori statistical model of the data and does not require training samples. However, the FCM

approach is computationally complex and is sensitive to noise. In the following section, we introduce the M-FCM technique to address these problems.

3. M-FCM algorithm

The standard FCM objective function for partitioning N feature vectors $\boldsymbol{x}_k$, $k \in [1,N]$, into c clusters is given by

$$J = \sum_{k=1}^{N} \sum_{i=1}^{c} u_{ik}^{p} ||\boldsymbol{x}_k - \boldsymbol{v}_i||^2, \tag{1}$$

where $\boldsymbol{v}_i$, $i \in [1,c]$, are the prototype signatures and the array $[u_{ik}] = U$ represents a partition matrix, $U \in \mathscr{U}$, namely

$$\mathscr{U}\left\{ u_{ik} \in [0,1] \,\middle|\, \sum_{i=1}^{c} u_{ik} = 1 \;\forall k \quad \text{and} \quad 0 < \sum_{k=1}^{N} u_{ik} < N \;\forall i \right\}.$$

The parameter p is a weighting exponent on each fuzzy membership and determines the amount of fuzziness of the resulting classification. Similar to the work of Bezdek et al. (1993), the FCM objective function is minimized when high membership values are assigned to the stack pixel whose signature is close to the centroid of its particular material signature, and low membership values are assigned when the stack pixel signature is far from the centroid. We modified Eq. (1) by introducing a term that allows the labeling of a stack pixel to be influenced by the labels in its immediate neighborhood. This neighborhood effect acts as a regularizer and biases the solution towards piecewise-homogeneous clusters. Such a regularization is useful in classifying images corrupted by salt and pepper noise. The modified objective function is given by

$$J_m = \sum_{k=1}^{N} \sum_{i=1}^{c} u_{ik}^{p} ||\boldsymbol{x}_k - \boldsymbol{v}_i||^2 + \frac{\alpha}{N_R} \sum_{i=1}^{c} \sum_{k=1}^{N} u_{ik}^{p} \left(\sum_{\boldsymbol{x}_r \in \mathscr{N}_k} ||\boldsymbol{x}_r - \boldsymbol{v}_i||^2 \right),$$

where $\mathscr{N}_k$ stands for the set of neighbours of $\boldsymbol{x}_k$ and N_R is the cardinality of $\mathscr{N}_k$. The neighbors effect term is controlled by the parameter α. The relative importance of the regularizing term is inversely proportional to the Signal to Noise Ratio (SNR) of the images. However, given a certain SNR value, there is no direct methodology to choose the optimal value of α to be used in this case. In general, lower SNR would require higher value of the parameter α. Formally, the classification problem comes in the form

$$\min_{U, \{\boldsymbol{v}_i\}_{i=1}^{c}} \quad J_m \qquad \text{subject to} \quad U \in \mathscr{U}. \tag{2}$$

The objective function J_m can be minimized in a fashion similar to the standard FCM algorithm. Taking the first derivatives of J_m with respect to u_{ik} and $\boldsymbol{v}_i$ and setting them to zero results in two conditions for J_m to be at a minimum. The constrained optimization in Eq. (2) is solved using Langrange multipliers

$$J_m = \sum_{k=1}^{N} \left(\sum_{i=1}^{c} \left(u_{ik}^{p} D_{ik} + \frac{\alpha}{N_R} u_{ik}^{p} \gamma_i \right) + \lambda \left(1 - \sum_{i=1}^{c} u_{ik} \right) \right),$$

where $D_{ik} = ||\boldsymbol{x}_k - \boldsymbol{v}_i||^2$ and $\gamma_i = \left(\sum_{\boldsymbol{x}_r \in \mathscr{N}_k} ||\boldsymbol{x}_r - \boldsymbol{v}_i||^2 \right)$. Taking the derivative of J_m w.r.t u_{ik} and setting the result to zero and then solving for u_{ik}, we have

$$u_{ik}^{*} = \left(\frac{\lambda}{p(D_{ik} + \frac{\alpha}{N_R}\gamma_i)} \right)^{1/p-1} \tag{3}$$

and since $\sum_{j=1}^{c} u_{jk} = 1 \;\forall k$, then

$$\sum_{j=1}^{c} \left(\frac{\lambda}{p(D_{jk} + \frac{\alpha}{N_R}\gamma_j)} \right)^{1/p-1} = 1$$

or

$$\lambda = \frac{p}{\left(\sum_{j=1}^{c} \left(\frac{1}{(D_{jk} + \frac{\alpha}{N_R}\gamma_j)} \right)^{1/p-1} \right)^{p-1}}.$$

Substituting λ into u_{ik}^*, the zero-gradient condition for the membership estimator can be rewritten as

$$u_{ik}^* = \frac{1}{\sum_{j=1}^{c} \left(\frac{D_{ik} + (\alpha/N_R)\gamma_i}{D_{jk} + (\alpha/N_R)\gamma_j} \right)^{1/p-1}}. \quad (4)$$

Similarly, solving for $\boldsymbol{v}_i$ we get

$$\boldsymbol{v}_i^* = \frac{\sum_{k=1}^{N} u_{ik}^p \left(\boldsymbol{x}_k + (\alpha/N_R) \sum_{\boldsymbol{x}_r \in \mathcal{N}_k} \boldsymbol{x}_r \right)}{(1+\alpha) \sum_{k=1}^{N} u_{ik}^p}. \quad (5)$$

The steps of the M-FCM algorithm can be summarized as follows:

Step 1. Read initial c signature prototypes $\{\boldsymbol{v}_i\}_{i=1}^{c}$.
Step 2. Update the partition matrix using Eq. (4).
Step 3. The prototypes of the signatures are obtained in the form of weighted averages of the patterns using Eq. (5).
Step 4. Repeat steps 2 and 3 until a convergence criterion is satisfied.

Usually the stopping criterion depends on the change in the partition matrix which leads to a large amount of calculation and long convergence time. In the M-FCM, the stopping criterion is when the values of the signature prototypes stabilize. This decreases the amount of computation needed and improves the convergence time substantially as shown in Fig. 2. Also the M-FCM converges to its stable state faster than the FCM, due to the field effect which increases or decreases the membership value with a higher rate than the FCM.

4. Results and discussions

Fig. 3 shows examples of spectral signatures of some substances taken from the US Geological Survey, Digital HYDICE Spectral Library: Version 4 (Clark et al., 1998). This library can be down-loaded from:

http://speclab.cr.usgs.gov/spectral.lib04/lib04H-YDICE.html. We tested the fuzzy hyperspectral classifier using HYDICE-generated, Desert Radiance II, hyperspectral sensor suite. The test image shown in Fig. 4 is a 210-channels stack and consists of five calibrated panels, each with a specific spectral signature. The image was classified into seven classes to accommodate both the grass and road materials. The figure shows the classification results using the M-FCM algorithm. These results are also shown in Fig. 5 in the form of a confusion matrix. We also generated fraction planes and abundance estimation for sub-pixel condition as shown in Fig. 5. This was done by mapping the membership score of each pixel relative to a given class for the entire input scene, and then

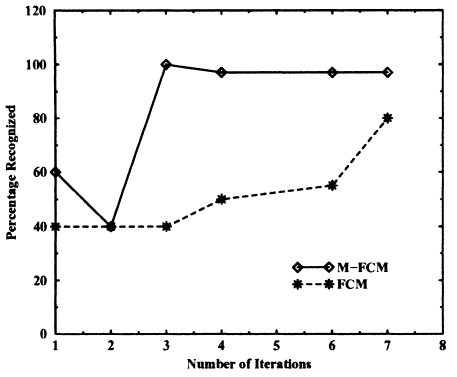

Fig. 2. A comparison between the FCM and the M-FCM in time and clustering rate using experimental data. Using the change in the signature values as a stopping criterion rather than the membership values improves the convergence time.

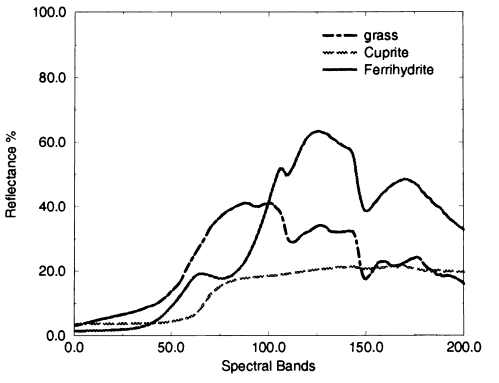

Fig. 3. Examples of spectral signatures of some substances taken from the US Geological Survey, Digital HYDICE Spectral Library: Version 4.

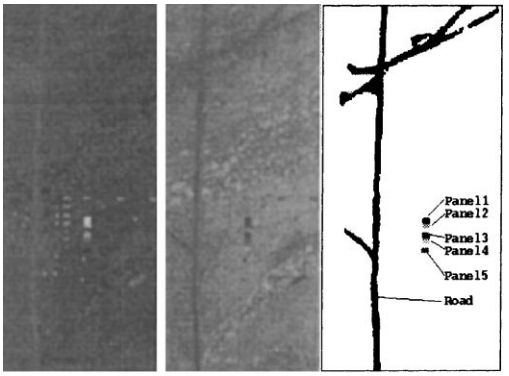

Fig. 4. Samples of a HYDICE-generated, Desert Radiance II, 210 channels hyperspectral stack. These samples are at different spectral wavelengths. The image consists of five calibrated panels each with a specific spectral signature. The last image shows the classification results.

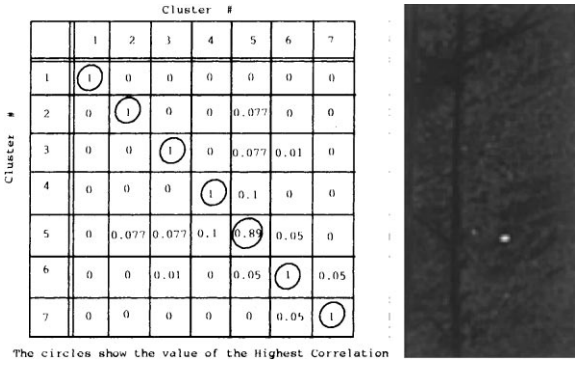

	1	2	3	4	5	6	7
1	1	0	0	0	0	0	0
2	0	1	0	0	0.077	0	0
3	0	0	1	0	0.077	0.01	0
4	0	0	0	1	0.1	0	0
5	0	0.077	0.077	0.1	0.89	0.05	0
6	0	0	0.01	0	0.05	1	0.05
7	0	0	0	0	0	0.05	1

Fig. 5. (left) A confusion matrix with the test data set. (right) Example of a fraction plane. We can see how the panel corresponding to the fraction plane cluster has the highest values, while other panels have disappeared. We can also see that part of the image has fractions that correspond to the cluster in study.

interpreting the resulting intensity value as an abundance estimator.

Comparison between the M-FCM, FCM and the Maximum Likelihood Classifiers (MLCs). To compare between the M-FMC, the traditional FCM and a statistical classifier, the MLC, Gaussian noise with different SNR was added to the test image. Fig. 6 compares the classification rates and false alarm rates of these classifiers. The comparison shows that the classification rate of

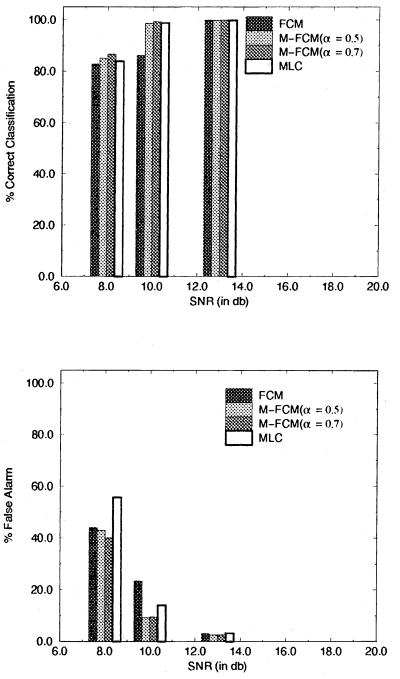

Fig. 6. % correct classification and false alarm using the FCM and the M-FCM algorithms. Different α values are used to illustrate its effect in case of low SNR.

the MLC and the fuzzy classifiers are the same for clear images. This gives an advantage to the fuzzy techniques since they do not require an a priori statistical model. However, in low SNR images, the FCM tends to be more sensitive to noise than the MLC and the M-FCM. Also the MLC gives a larger false alarm rate with low SNR images than the M-FCM. This was expected since the M-FCM is the only technique that considers the target field rather than individual pixels in the classification. In general, the comparison shows the superiority of the M-FCM, especially with low SNR.

M-FCM parameters selection. Fig. 6 shows that the M-FCM with a larger value of α performs better in case of low SNR images. However, in noise-free images, the FCM (M-FCM with $\alpha = 0$) has the same performance as the M-FCM with a large value of α, while the later increases the operations complexity. This leads to the problem of the proper choice of the M-FCM parameter α. Also, for low SNR images, this parameter α has an

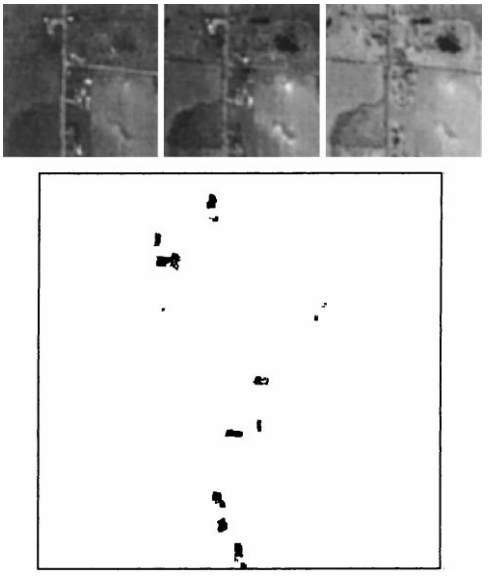

Fig. 7. Another example of samples of hyperspectral stack at different spectral wavelengths. The result of applying the fuzzy hyperspectral classifier is shown at the bottom. Each classified region represent an ROI where a man-made object is detected. A fuzzy belief value is associated with each ROI.

effect similar to the learning-rate parameter in neural network learning. The smaller this parameter is, the longer it takes to reach a stable solution. Increasing the value of this parameter on the other hand leads to blurring the object edges. Heuristics methods that can be used to carefully select this parameter will be similar to those used in selecting the learning-rate parameter in neural network learning.

Fig. 7 shows an example of using the hyperspectral classifier in detecting and identifying ROIs in a 16-channel hyperspectral stack. Each one of the ROIs is associated with a fuzzy value corresponding to a certain material signature. This fuzzy value is used as a belief measure in the next stage of the ATR system as described by Mostafa et al. (1999).

5. Conclusions

In this paper we described a fuzzy-based hyperspectral classifier for automatic target identification. A modified fuzzy C-Means (M-FCM) clustering algorithm was used in this classifier. The results show that the classifier was capable of clustering hyperspectral data starting from a known spectral signature library. We used simulated lab-based spectral curves and applied it to a HYDICE-generated, Desert Radiance II, hyperspectral stack. The results showed that the fuzzy hyperspectral classifier is successful in target identification using materials spectrum. It has the advantages of being used with any number of features and any number of classes. Also it provides a fuzzy belief value that can be used later in the decision-making stage.

Discussion

Raghavan: It looks to me that this smoothing could also be used for analysing stock market data.

Farag: The question is: can the fuzzy C-means algorithm be used to cluster other data, and the answer is yes; for instance, we have used it for MRI-data segmentation. As you know, a statistical approach to clustering can be used as well. The fuzzy C-means is just one approach that happened to work nicely for hyperspectral data classification.

Gimel'farb: I have two questions. First of all, the spectral signature from a real target is not only influenced by statistical variance, but also by the fact that there is no pure material in this case. For instance, if the hidden target is a tank, it will be hidden by grass, by dirt, by water maybe, so you will obtain some joint signature. How do you use the library of materials to detect it in such a case?

Farag: This is an excellent question. That is the reason why stochastic and fuzzy classifiers are used to solve this problem. The fuzzy C-means algorithm is capable of identifying "partial" pixels, belonging to more than one material. The algorithm gives a fuzzy value for each material, for instance 0.3 water and 0.7 steel. This is used later on in the decision making phase of the ATR system.

Gimel'farb: Thank you. The second question is: in an ideal situation, with cars such as shown in

your presentation, why do you need some fuzzy description? I would think that you can find some monotonic transformation to go from one to another. So the usual dynamic programming techniques could be used to find the best match in the library.

Farag: Well, I know that you have a lot of experience with dynamic programming, it might work as well. People have used deterministic and statistical approaches for this problem. But since we are not dealing with "ideal" situations, statistical and fuzzy approaches are more appropriate. As a matter of fact, I will ask my students to compare the Fuzzy C-means with all these approaches. They are all easy to program, and maybe we can include dynamic programming as well.

Zheng: I just wonder, how could you use this method for general cases? You may want to detect some target you have not seen before.

Farag: Remember that in our application, the database is not very large. We are after specific things: tanks, trucks, and other specific targets. All this is put into the context of this application. I am not trying to solve a very general problem. Because of this, and because of the constraints that are surrounding it, the database is very limited. As a result, their search is not so much of a problem, and speed is not really a concern in this case. On the other hand, in applications such as speech identification, for example, where you have a large dictionary, then you are right. Then you have a computation problem.

Zheng: So the major application of your system is verification, rather than the detection of unknown objects?

Farag: It could be used for detection, and verification as well.

Zheng: But this fuzzy C-means procedure only allows you to do a mapping to a library. For unknown objects, you cannot perform such a mapping. So, verification is possible, unknown objects detection is something else.

Farag: In the ATR language, verification means a need to define: is this a tank, and if it is, is it a Russian tank, an American tank, what brand, and so on. So you have a hierarchy of classification. We do not just use fuzzy C-means to solve the whole verification problem. In the sensor fusion paradigm for target identification, we use the target (material) signature as one element in the process. Yes, if the object has unknown material, the algorithm will produce a false detection. However, we are currently using a well-known hyperspectral library, available on the Internet, that contains almost all known material spectral signatures.

Acknowledgements

This work has been partially supported by grants from the US Dept. Of Defense under contract: USNV N00014-97-11076.

References

Basedow, R.W., Armer, D.C., Anderson, M.E., 1995. HYDICE system: Implementation and performance. SPIE Proc. 2480, 258–267.

Bezdek, J., Hall, L., Clarke, L., 1993. Review of MR image segmentation using pattern recognition. Medical Phys. 20, 1033–1948.

Burrough, P.A., MacMillan, R.A., Van Deursen, W., 1992. Fuzzy classification methods for determining land suitability from soil profile observations and topography. J. Soil Sci. 43, 193–210.

Chulhee, L., Landgrebe, D.A., 1993. Decision boundary feature extraction for non-parametric classification. IEEE Trans. System, Man. Cybernet. 23 (2), 433–444.

Clark, R.N., Swayze, G.A., King, T.V.V., Gallagher, A., Calvin, W.M., 1998. US Geological Survey, MS 964, Box 25046, Federal Center Denver, CO 80225-0046.

Hsu, S-Y., Huang, C-Y., 1997. Concealed fixed object detection with hyperspectral data in SRE's IMaG Environment. In: Proceedings of SPIE, International Conference on Imaging Spectrometry III, Vol. 3118. pp. 69–80.

Landgrebe, D.A., 1999. Information extraction principles and methods for multispectral and hyperspectral image data. In: Chen, C.H. (Ed.), Chapter 1 of Information Processing for Remote Sensing. World Scientific, River Edge, NJ, USA.

Mohamed, N.A., Ahmed, M.N., Farag, A.A., 1998. Modified fuzzy C-mean in medical image segmentation. In: Proc. of IEEE-EMBS, Hong Kong, Vol. 20, No. 3, pp. 1377–1380.

Mostafa, M.G., Hemayed, E.E., Farag, A.A., 1999. Target recognition via 3D object reconstruction from image

sequence and contour matching. Pattern Recognition Letters 20 (11–13), 1381–1387.

Ratches, J.A., Walters, C.P., Buser, R.G., Guenther, B.D., 1997. Aided and automatic target recognition based upon sensory inputs from image forming systems. IEEE Trans. Pattern Anal. Machine Intell. 19 (9), 1004–1019.

Slater, D., Healey, G. 1998. Exploiting an atmospheric model for automated invariant material identification in hyperspectral imagery. In: Proc. SPIE, Algorithms for Multispectral and Hyperspectral Imagery IV, Sylvia S, Vol. 3372. pp. 60–143.

Vane, G., Green, R.O., Chrien, T.G., Enmark, H.T., Hansen, E.G., Porter, W.M., 1993. The airborne visible infrared/imaging spectrometer (AVIRIS). Remote Sensing of the Environment 44, 127–143.